

# EXPERIMENTAL INVESTIGATION OF RESPONSE OF STEEL TUBULAR COLUMNS TO CLOSE RANGE EXPLOSIONS

Alex Remennikov<sup>1</sup>, Brian Uy<sup>2</sup>, Igor Mentus<sup>3</sup>

**ABSTRACT:** *This paper describes the blast loading trials on steel tubular members with and without concrete infill. The standoffs considered in this trial were selected to demonstrate the response of these steel sections to contact and very close-range detonations of high explosive (HE). The main objective of the trials was to investigate the effects of contact and near-field explosions on steel square tubular members and to demonstrate the effect of standoff variation on the mode of response and failure of steel square sections. The experimental data collected during these trials can be used for verification of theoretical and numerical models of response of steel tubular columns subjected to contact and close-range blasts. Due to difficulties with collecting quantitative data (displacements, blast pressures etc.) in the close proximity of a detonating HE charge, analysis of the steel tubes in this paper is confined mostly to qualitative assessment based on visual observations of the structural damage and limited numerical simulations of the blast-structure interaction aiming at clarifying some important phenomena that were not available to be obtained directly from the explosive tests. A new simplified approach to predicting the dynamic response of square tubular steel members subjected to the near-field airblast loading is proposed.*

**KEYWORDS:** Blast, near-field detonation, steel columns, structural damage

---

<sup>1</sup>Alex Remennikov, Faculty of Engineering, University of Wollongong. Email: alexrem@uow.edu.au

<sup>2</sup>Brian Uy, Centre for Infrastructure Engineering, University of New South Wales. Email: b.uy@unsw.edu.au

<sup>3</sup>Igor Mentus, School of Military Engineering, Kamenetz-Podolsk National University, Ukraine, Email: mentus\_vii@rambler.ru

# 1 INTRODUCTION

Response of structural systems and elements to the blast resultants generated by a distant external explosion have been investigated thoroughly and a number of publicly accessible design guidelines, manuals and monographs are available for conducting blast vulnerability assessment studies and designing protective structures [1,2]. However, response of structural components to contact and close-range detonations of high explosives (HE) has not been investigated to the level sufficient for developing engineering-level design and analysis tools and producing reliable design recommendation.

One of the characteristic scenarios, where knowledge and understanding of the blast environment caused by contact and close-range HE detonation could be critical, involves malevolent attack on primary load carrying elements of buildings, bridges and other infrastructure facilities. Even a relatively small explosive device delivered in a bag or backpack and left in a close proximity to a building column or bridge pier could cause severe localized damage and consequent partial collapse of the infrastructure. This is arguably the most difficult area of blast engineering for studying both experimentally and analytically, where classical shock wave measurement and modelling techniques would be ineffective due to the loading being dominated by the impingement of dense, high-pressure, high-temperature detonation products rather than a diffracting shock wave, and absence of reliable material models and equations of state.

Response of square tube steel beams to impulsive loading was investigated by Wegener and Martin [3]. The beams were simply-supported and made up of hollow mild-steel box square section with dimensions  $25 \times 25$  mm. Sheet explosive was used to provide a uniformly distributed impulse over the full span. The results of the impulsive loading tests confirmed that the box section experiences two modes of deformation. Firstly, a local deformation mode transforms the cross-section of the beam from its rectangular shape to a shape in which the top half of the section undergoes significant plastic deformation. Secondly, the beam undergoes a global beam mode-type deformation. An important suggestion that follows from that study is about timing of occurrence of the two mechanisms. The analysis confirmed that the characteristic times for the two mechanisms of deformation are different by at least an order of magnitude, thus suggesting that the two mechanisms can be considered as sequential and uncoupled for the purpose of an approximate rigid-viscoplastic analysis of the cross-section. Since this study used a uniformly distributed impulse over the beam span, these findings cannot be extended directly to cases where

a square steel tubular beam or column is subjected to a concentrated impulse due to contact or close-in detonation of high explosive charges.

The failure modes and analytical prediction of the response of the hollow and concrete-filled steel square tubular sections subjected to a highly localized blast impulse have not been studied yet, to the best of the authors' knowledge. This paper presents the results of explosive trials on the steel square tubular columns subjected to the near-field blast loading effects. The experimental data are then used to validate a simplified engineering-level analysis of concrete-filled steel tubular members subjected to a large-magnitude concentrated blast impact caused by a close-in detonation of HE charges.

## 2 NEAR-FIELD BLAST LOADING

The sudden expansion of initially highly compressed explosion products generates the blast wave. Two types of blast waves are generated in a conventional explosion. One is a close-in composite blast wave that includes both detonation products and air; and the other one is a more distant blast wave that involves atmospheric air only. The propagation of a blast wave can be broken down into four regimes; (1) the detonics, (2) near-field, (3) mid-field, and (4) far-field regimes. An evolution from the detonics to the near-field regime is illustrated in Figure 1. The two types of blast waves can be described in terms of a reference explosion for which Kinney [4] suggested using a bare spherical charge of TNT due to availability of analytical solutions [5] and significant body of experimental measurements [6].

### 2.1 PHYSICS OF NEAR-FIELD BLAST

In this paper, the response of structures to the near-field blast regime of loading is investigated. In the near-field, the structural loading is dominated by the impingement of detonation products. Initial pressure within the detonation products is detonation pressure. For TNT, maximum detonation pressure is about 21 GPa at typical density of  $1650 \text{ kg/m}^3$ , or about 15 GPa at density of  $1500 \text{ kg/m}^3$  which was the actual density used in this study. The central portion of the detonation products cloud stays in place, and the pressure in the centre decreases following the isentropic pressure-volume relation as the fireball of detonation products expands. Kinney [4] summarized the pressure regions based on the profile of composite blast wave shown in Figure 1. Direct explosion pressures extend out to distances up to 1.6 charge radii from explosion centre with peak overpressures around 30-35 MPa for the reference explosion (a bare spherical charge of 1 kg

TNT). The region of composite blast extends out to about 15 charge radii, with peak overpressures varying from 35 MPa to 1.2 MPa. Simple air blast starts at distances greater than 15 charge radii where peak overpressures are less than 1.2 MPa for the reference explosion.

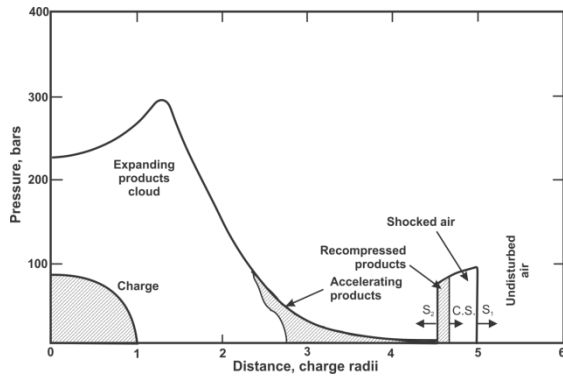


**Figure 1:** Profile of composite blast wave

## 2.2 EXPLOSION TRIALS

The aim of the blast loading trials was to investigate experimentally the response and failure modes of steel square hollow and concrete-filled square hollow sections subject to contact and close-range detonations of HE charges. Table 1 presents the testing program and the variables examined in the tests. All columns were 100x5 SHS Grade 350 steel tubular sections.

**Table 1:** Testing program summary

Test	Specimen	Column design	Charge (kg)
1	C1	concrete filled	2.610
2	C2	concrete filled	2.600
3	C3	hollow	2.603
4	C4	concrete filled	2.605
5	C5	concrete filled	2.610

## 2.3 MATERIAL PROPERTIES

Sample tensile specimens from the 100x5 SHS columns were tested until failure in the Instron 8033 universal testing machine. The mean yield stress of the steel in tension from the 100x5 SHS columns was found to be 424 MPa. These values demonstrated a significant increase from the nominal value  $f_y = 350\text{MPa}$ , specified by the supplier. The average ultimate tensile strength of the steel recorded was 470 MPa for the 100x5 SHS sections. The mean values obtained from these tests will be used for the theoretical analysis and numerical simulations of the columns specimens in this study. The Strength Increase Factor (SIF) is required in blast-resistant design of steel elements to take into consideration the true yield strength capacity. Based on the material tests data, the SIF =

$424\text{MPa}/350\text{MPa} = 1.21$  will be used in the blast analyses of the tubular columns.

Throughout the experimental investigation of the column specimens concrete testing was periodically conducted. The aim of this testing was to determine the characteristic compressive strength of the concrete used as the infill material in the composite columns. Five cylinders were tested several days before the explosive trials and the average compressive strength was determined to be 46 MPa. This average compressive strength of the concrete will be used for the theoretical analysis and numerical simulations of the columns specimens in this study.

Five steel square tubular specimens were prepared for the explosive testing. The square tubular columns used cold-formed structural hollow steel sections 100x5 SHS Grade C350 from OneSteel with 200 PFC steel channel sections and concrete end blocks forming the column specimens. The end concrete blocks had dimensions 250 mm (W) x 350 mm (D) x 400 mm (H) and were designed to provide additional inertial resistance to the specimens in order to avoid excessive rebound reaction of the specimens. The column specimens had a clear span of 2.0 metres between the end blocks. The geometry and section details of the column specimens are shown in Figure 2. The columns were tested in a horizontal position and were supported by means of the concrete blocks with the embedded steel channel sections welded to the ends of the columns. The concrete end blocks were free-standing on the ground and could rotate in response to large columns deformations. Hence, the horizontal column specimens were assumed to act as simply supported beams under blast loading. The ground clearance was 250 mm.

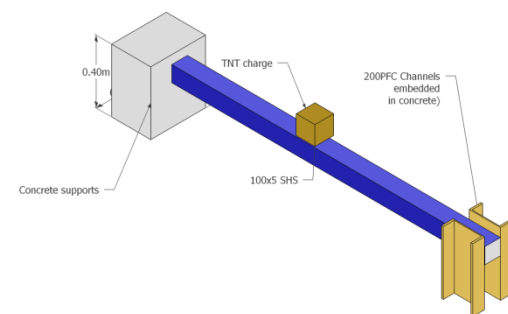


**Figure 2:** Experimental setup for blast testing

The explosive load was provided by a square charge of trinitrotoluene (TNT) placed either directly in contact with the column surface or at the appropriate standoff above the column surface. The required standoff distances were created using the polystyrene spacers. TNT charges were prepared by casting molten TNT into 120 mm cubic moulds. Pentolite booster, with integral detonator well, was cast into the TNT cube charges to facilitate charge detonation centrally from the

top. An average actual density of TNT was 1500 kg/m<sup>3</sup> with an average mass of the explosive charges of 2.6 kg. All explosive charges were detonated using electric initiation system. Figure 3 shows the fireball caused by detonation of the cubic TNT charges in the live tests discussed in this paper.



**Figure 3:** Fireball during column testing

### 3 EXPERIMENTAL RESULTS

#### 3.1 COLUMN C1

Column C1 was tested by placing the cubic TNT explosive charge on the top surface of the square steel section and initiating it from the top using the electric #8 detonator. The column specimen C1 failed in a catastrophic failure mode by splitting in half and forming severely deformed column remains as shown in Figure 4.



**Figure 4:** Demolition of Column C1

#### 3.2 COLUMN C2

The effect of small air gap between the explosive charge and the concrete-filled steel section was investigated by placing the cubic TNT charge 50 mm above the top surface of the column. The charge was initiated centrally from the top using electric detonator. Figure 5 presents the localised demolition of the specimen. One can observe a noticeable difference in the failure modes of columns C1 and C2. Column C2 was breached by the blast but it did not cause a ‘peeled banana’ destruction of the column. This demonstrates a significant effect of a small air gap between the

charge and the structure in reducing the intensity of loading by the detonation products for the ‘near-field’ loading regime. No direct measurements were performed in this test due to the severe blast loading environment produced by the HE detonation in close proximity from the specimen.



**Figure 5:** Demolition of Column C2

#### 3.3 COLUMN C3

Column C3 was square hollow section without concrete infill. It was subjected to an explosion resulting from the cubic TNT charge positioned above the column top surface at a distance of 100 mm with the polystyrene spacers. The charge was detonated from the top using the electronic detonation system. The failure mode of column C3 is shown in Figure 6. It can be observed from Figure 6 that the column experienced global large flexural deformation and localised breaching failure of the tube top and bottom walls. This explosion can be classified as the ‘near-field’ gasdynamic regime characterised by the fireball engulfing the column and impinging high-pressure detonation gases. The close-up view of the central zone of the column shown in Figure 6 clearly illustrates severe outward plastic deformations of the vertical walls of the tube caused by the detonation gases.



**Figure 6:** Demolition of Column C3



### 3.4 COLUMN C4

In order to have a direct comparison between the failure modes of hollow and concrete-filled square sections, column C4 had the concrete infill and was tested at the same standoff distance as for column C3 which used the hollow tube section. The cubic TNT charge was placed 100 mm above the top face of the column using the polystyrene spacers. The charge was detonated from the top. The failure mode of column C4 is presented in Figure 7. Figures 6 and 7 give an opportunity for a qualitative analysis of the response of steel square tubes with and without concrete infill when subject to the near-field regime of explosive loading. One can notice that both types of the columns experienced a combination of global plastic flexural response and severe localised plastic deformation of the central zone. The concrete-filled section was not breached by the blast unlike the hollow section subjected to the same explosive loading. Severe plastic rotation and large plastic outward deformations of the tube walls render this column member unusable with no residual capacity for resisting gravity loads. The maximum displacement of the column was greater than 250 mm since the column rotation was terminated by the ground surface.



**Figure 7:** Large plastic deformation of Column C4

### 3.5 COLUMN C5

The standoff distance was further increased to 150 mm for column C5 to investigate the response of the concrete-filled steel square tube. The blast environment at this standoff is still categorized as 'near-field' regime with the explosive loading generated predominantly by the engulfment of the column by the products of detonation. The cubic TNT charge was placed 150 mm above the top surface of the specimen using the polystyrene spacers. The charge was initiated from the top using electric detonator. The failure mode of column C5 is presented in Figure 8. Comparison of the blast response and failure modes for columns C4 and C5 in Figures 7 and 8 demonstrates a remarkable improvement in the performance of the

concrete-filled tube following the increase in scaled standoff distances from  $0.08 \text{ m/kg}^{1/3}$  to  $0.12 \text{ m/kg}^{1/3}$ . The maximum residual displacement was about 152 mm, which is significantly less than that for column C4. The column cross-section near the centre was severely compressed, but the concrete infill seemed to have provided an internal support to the tube walls and prevented steel rupture, breaching failure as well as local buckling failure of the tube walls at the mid-span.



**Figure 8:** Plastic deformation of Column C5

## 4 ANALYTICAL MODELING FOR NEAR-FIELD BLAST LOADING

### 4.1 HYPOTHESIS OF INSTANTANEOUS DETONATION

When analysing mechanical effects of explosion, as a first approximation, it is possible not to take into consideration the detonation velocity of the explosive charge, i.e. to make an assumption about the instantaneous nature of explosive charge detonation.

For explosion in air, the air pressure is insignificant compared to the detonation pressure, as such it is possible to neglect the pressure of the surrounding air at the initial phase of expansion of detonation products. For very close distances from the explosive charge (10-15 radii of the charge), the density of the surrounding medium may also be disregarded since its value is 700-800 times lower than that of the density of the explosive material. For more distant explosions, the density of air will be of higher importance since its density will be comparable to the density of expanded disturbed field of detonation product gases.

These are the main simplifying assumptions that are used to derive the analytical expressions of explosive loading on structural elements for close-range explosions. They can also be summarised as follows:

1. Detonation process is instantaneous (i.e. assume detonation velocity  $D \rightarrow \infty$ );

2. The pressure  $p_1$  of the surrounding medium is insignificant compared to the pressure of the detonation product gases and may be neglected (i.e. assume  $p_1 \rightarrow 0$ );
3. The density  $\rho_1$  of the surrounding medium is very small compared to the density of the detonation product gases (i.e. assume  $\rho_1 \rightarrow 0$ ).

According to the last two assumptions ( $p_1 \rightarrow 0$ ,  $\rho_1 \rightarrow 0$ ), the surrounding medium is not present and only the detonation product gases contribute to the one-dimensional flows in the disturbed region surrounding the explosive charge. The proposed formulas shall be used with a clear understanding of the made assumptions. If the problem formulation demands conditions that are significantly different from the simplifying assumptions, other more precise (but more demanding) analytical or computational techniques should be used.

Under the condition of instantaneous detonation, all explosive charge particles are stationary because initially they hold the volume of the original explosive. After the instantaneous explosion, the detonation product gases begin to expand. The particles located on the outer surface of the charge begin flying away first. Following the outer surface particles, the particles located on the successive interior surfaces start progressively flying away so that the boundary between the moving particles and the stationary particles is moving inside the charge with some velocity. This velocity can be termed *the velocity of outburst surface* and the moving boundary - *the outburst surface*. It is noteworthy that in the real process of detonation the disturbances move back inside the detonation products with the velocity of sound in the detonation products, and the boundary of this disturbance is the head of the rarefaction wave where the explosion parameters vary smoothly. The assumption of an instantaneous detonation and hypothetical outburst surface provide sufficiently accurate solution for the blast parameters in the surrounding medium only for the region within 10-15 charge radii from the charge. Figure 9 shows a general picture of outflow of explosion products.

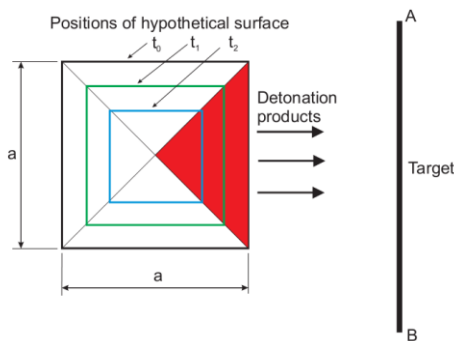


**Figure 9:** Hypothetical outburst of detonation products for cubic HE charge

## 4.2 DETERMINATION OF IMPULSE DUE TO NEAR-FIELD EXPLOSION

First, we assume that the impulse  $I$  is produced by detonation of a spherical charge of mass  $W$  and radius  $r_0$ , placed over the mid-span of a beam at a standoff distance  $a$ , as shown Figure 10. Then, for the near-field condition  $a/r_0 < 15$  and employing the hypothesis of instantaneous explosion [7], it can be shown that the specific impulse,  $i$ , can be expressed as

$$i = \frac{A_0 W}{a^2} \cos^4 \alpha \quad (1)$$

where  $A_0 = (u_0 + w_0)/4\pi$ ,  $u_0$  is the particle velocity of the detonation products,  $w_0$  is the velocity of the hypothetical outburst surface, and  $\alpha$  is the angle explained in Figure 10.

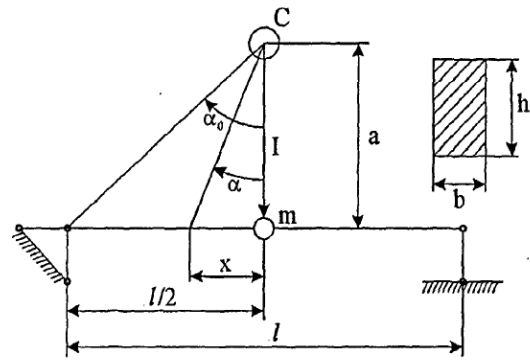


**Figure 10:** Calculation of blast impulse on beam

Assuming that the beam has a rectangular cross-section with the dimensions  $b$  (breadth) and  $d$  (depth), the specific impulse per unit length of the beam can then be determined as

$$i_* = i \times b \quad (2)$$

and the total impulse acting on an elementary beam segment  $dx$  can be written as

$$dI = i_* dx = \frac{A_0 W b}{a^2} \cos^4 \alpha dx \quad (3)$$

Further, taking into consideration that  $x = a \tan(\alpha)$ , Equation (3) can be re-written as

$$dI = \frac{A_0 W b}{a} \cos^2 \alpha d\alpha \quad (4)$$

After integrating Equation (4) and considering the beam and charge location symmetry, we get the expression for the total impulse acting on the beam as follows

$$I = 2 \int_0^{\alpha_0} dI = \frac{A_0 W b}{a} \left( \alpha_0 + \frac{1}{2} \sin 2\alpha_0 \right) \quad (5)$$

where  $\alpha_0 = \arctan(l/2a)$  (see Figure 10). The total impulse,  $I$ , determined from Equation (5), can be used to determine the initial beam velocity due to a near-field explosion.

### 4.3 NON-UNIFORM DISTRIBUTION OF IMPULSE ALONG BEAM

A simplified approach to calculating the impact impulse for the near-field airblast regime and applying it in a non-uniform fashion on the structure is developed in this section. To determine the non-uniform distribution of the specific impulse along the beam element, we need to find an expression for  $i_*(\xi)$ , where  $\xi$  is the position along the beam such that  $0 \leq \xi \leq l/2$ . From Figure 10, it can be shown that the angle of incidence,  $\alpha$ , can be expressed as follows

$$\cos^2 \alpha = \frac{a^2}{a^2 + \left(\frac{l}{2} - \xi\right)^2} = \frac{a^2}{l^2 \left( \frac{a^2}{l^2} + \left(\frac{1}{2} - \frac{\xi}{l}\right)^2 \right)} \quad (12)$$

Therefore, substituting Equation (12) into Equation (1) yields the following expression for the specific impulse per unit length of the beam for the near-field blast flow regime

$$i_* = \frac{A_0 W b}{a^2} \frac{a^4}{l^4 \left[ \frac{a^2}{l^2} + \left(\frac{1}{2} - \frac{\xi}{l}\right)^2 \right]^2} \quad (13)$$

Using the relationship between the specific impulse per unit length and the position along the beam,  $\xi$ , given by Equation (13), one can calculate the spatial distribution of the positive phase duration impulse and the associated magnitudes of the initial velocities for the segments of the structural element. The values of initial velocities are then assigned to the corresponding nodes of the finite element model to model the effect of blast impulse on the structural component. Figure 11 shows the predicted distribution of the initial velocities for column specimen C5 where the explosive charge is positioned at a scaled standoff distance of  $0.15 \text{ m/kg}^{1/3}$ . From the graph in Figure 11 it is clear that more than 80 percent of the total explosive energy is applied over the centrally located segment extending about 200 mm both sides from the mid-span. This observation justifies using the beam with a concentrated load model for the derivation of the

equivalent SDOF system for modelling the near-field blast response of structural elements.

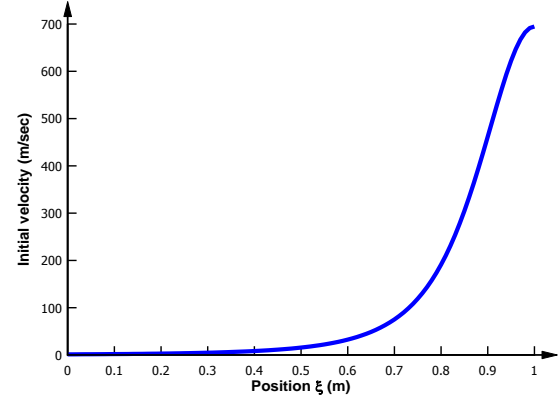


**Figure 11:** Initial velocities along half-span for Column C5

## 5 LS-DYNA MODELLING

LS-DYNA, a general purpose transient dynamic finite element program [8] was used to develop the finite element models in this study. LS-DYNA is used to solve multi-physics problems including solid mechanics, heat transfer, and fluid dynamics either as separate phenomena or as coupled physics, e.g., thermal stress or fluid structure interaction. LS-DYNA is industry accepted dynamic first-principle based code for analysis of structures under extreme loads generated by blast and impact events with the ability to compute large deformations due to flexure, shear, and material failures.

The LS-DYNA finite element model of column specimen C5 with the initial velocities is shown in Figure 12(a). The model includes the steel square tubular section 100x5 SHS modelled using Belytschko-Tsay shell elements. The concrete infill is modelled using constant stress solid elements. The steel square tube is modelled rigidly connected to the upstanding steel channel PFC sections, which is also modelled using shell elements. From the convergence study, a mesh size of 10 mm was found to be appropriate for the steel sections and the concrete core.

The concrete blocks at each end of the specimen shown in Figure 2 were not included in the model for the sake of model simplicity and because their primary role was to increase inertial resistance of the tested steel tubular members. To consider the effect of the concrete blocks, the material density of the steel channels in the model can be increased to match the total mass of the end supports in real tested structures.

In the real test conditions, the supporting blocks were standing on the ground and free to rotate and move in the upward direction. To simulate the similar boundary conditions, a ground plane was

defined using LS-DYNA keyword \*RIGIDWALL\_PLANAR with the rigid wall's origin defined at the level of the bottom edge of the steel channel sections.

The initial velocity conditions were applied to the nodes on the top surface of the steel tubular member as shown in Figure 12(a). The nodes across the width of the element were grouped in the node sets and assigned the initial velocities using \*INITIAL\_VELOCITY command in LS-DYNA. The peak value of the initial velocity assigned to the nodes at the mid-span was 700 m/sec. Using the mesh size of 10mm and the graph in Figure 11, the initial velocities were estimated and assigned to the node sets on the top surface of the steel tube.

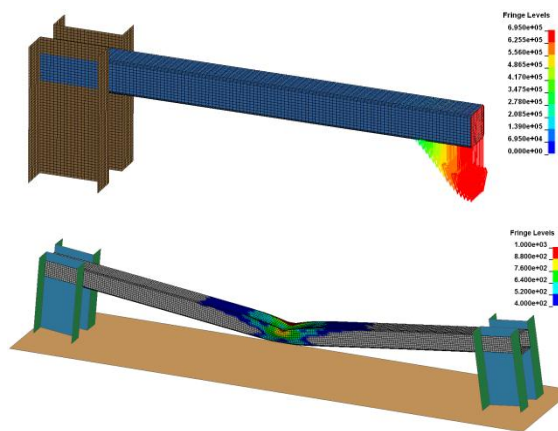


**Figure 12:** (a) LS-DYNA model of Column C5 with initial velocities applied; (b) Numerical prediction of blast damage to Column C5

The blast damage of column C5 as predicted by the LS-DYNA model is presented in Figure 13. The results of numerical simulations can be qualitatively compared to the damage experienced by the specimen in the explosive test as shown in Figure 8. It can be noticed that numerically predicted deformation mode is very similar to the one observed in the explosive tests.

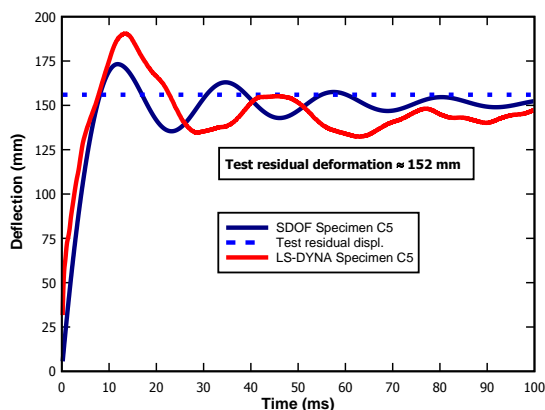


**Figure 13:** Comparison of numerical predictions and experimental deformations for column C5

Plotting the time histories of the mid-span vertical displacements and comparing them with the SDOF predictions [9] of the column response to the near-field blast impulse in Figure 13, provides an opportunity to validate these techniques against the test residual deformation values. One can see that the three techniques provided very similar final damage predictions thus validating the simplified SDOF modelling and 3-D FEA non-linear modelling. The peak dynamic displacements predicted by the LS-DYNA model turned out to be higher than that from the SDOF analysis by about 10% with the peak deformations occurring at approximately the same time instances after the initiation of the detonation. These findings corroborate the validity of simplified engineering techniques based on sound principles of blast physics and equivalent system transformation for predicting response of structural elements to near-field blast regime loading.

## 6 CONCLUSIONS

This study has shown that simplified analytical modelling of near-field blast effects combined with modelling dynamic structural response using FE non-linear analysis can form a basis for the development of an engineering-level approach for predicting response of structures to close-in detonations of HE charges. It was demonstrated that utilising the assumption of an instantaneous detonation, the specific impulse for an explosion occurring at a short distance from a rigid obstacle can be predicted and used for the determination of the initial conditions for FE-based dynamic analyses. In this case, a structural member is analysed to the effect of a concentrated blast impact impulse inflicted by the shock wave rather than carrying out a highly complicated coupled Arbitrary Lagrange Euler (ALE) blast wave – structure interaction analysis for close-range HE detonations.

## ACKNOWLEDGEMENT

The authors would like to thank the technical staff at the structural laboratories of the University of Wollongong and the University of Western Sydney for assisting with manufacturing the specimens and conducting the experiments. The authors also thank Messrs. Steve Courtney and Marcus Erasmus of Applied Explosives Technologies Pty Ltd for technical assistance with explosive testing. Special thanks go to Mr David Ritzel of Dyn-FX Consulting Ltd., Canada for extremely useful discussions of physics of near-field explosions. This project was sponsored by an ARC Discovery Near Miss Grant in the School of Engineering at the University of Western Sydney, and this support is gratefully acknowledged.



## REFERENCES

- [1] Department of Defence. UFC 3-340-02 Structures to Resist the Effects of Accidental Explosions. 2008, Washington, D.C.
- [2] Krauthammer, T. Modern Protective Structures. CRC Press, Taylor and Francis Group, 2008.
- [3] Wegener R.B and J.B. Martin. Predictions of permanent deformation of impulsively loaded simply supported square tube steel beams. Int. J. Mech. Sci. 1985; 27(1-2): 55-69.
- [4] Kinney G. F. Engineering Elements of Explosions. Naval Weapons Centre, China Lake, California, November, 1968.
- [5] Brode, H. L. Numerical solutions of spherical blast waves. J Appl Phys 1955; 26: 766.
- [6] Kingery C. N. Air Blast Parameters versus Distance for Hemispherical TNT Surface Bursts. BRL Report No. 1344, Aberdeen Proving Grounds, September, 1966.
- [7] Salamakhin, T. M: Effect of explosion on structural elements, Moscow, Military Engineering Academy Publication, 1969 (in Russian).
- [8] LS-DYNA Version 971, Livermore Software Technology Corp., Livermore, CA, May 2008.
- [9] Remennikov A.M. and Uy B. Simplified Modeling of Hollow and Concrete-Filled Square Tubular Steel Columns for Near-Field Detonations. In: *The 15th International Symposium on the Interaction of the Effects of Munitions and Structures (ISIEMS15)*, Potsdam, Germany, September 17-20, 2013.